Cosimo Bambi *Editor*

Tutorial Guide to X-ray and Gamma-ray Astronomy

Data Reduction and Analysis

Springer

Tutorial Guide to X-ray and Gamma-ray Astronomy

Cosimo Bambi
Editor

Tutorial Guide to X-ray and Gamma-ray Astronomy

Data Reduction and Analysis

Springer

Editor
Cosimo Bambi
Department of Physics
Fudan University
Shanghai, China

ISBN 978-981-15-6336-2 ISBN 978-981-15-6337-9 (eBook)
https://doi.org/10.1007/978-981-15-6337-9

© Springer Nature Singapore Pte Ltd. 2020
This work is subject to copyright. All rights are reserved by the Publisher, whether the whole or part of the material is concerned, specifically the rights of translation, reprinting, reuse of illustrations, recitation, broadcasting, reproduction on microfilms or in any other physical way, and transmission or information storage and retrieval, electronic adaptation, computer software, or by similar or dissimilar methodology now known or hereafter developed.
The use of general descriptive names, registered names, trademarks, service marks, etc. in this publication does not imply, even in the absence of a specific statement, that such names are exempt from the relevant protective laws and regulations and therefore free for general use.
The publisher, the authors and the editors are safe to assume that the advice and information in this book are believed to be true and accurate at the date of publication. Neither the publisher nor the authors or the editors give a warranty, expressed or implied, with respect to the material contained herein or for any errors or omissions that may have been made. The publisher remains neutral with regard to jurisdictional claims in published maps and institutional affiliations.

This Springer imprint is published by the registered company Springer Nature Singapore Pte Ltd.
The registered company address is: 152 Beach Road, #21-01/04 Gateway East, Singapore 189721, Singapore

Preface

X-ray and γ-ray astronomy, namely, the study of astrophysical objects in the X-ray and γ-ray bands, began in the early 1960s and opened a new window for the study of violent phenomena in the Universe. In the past 20 years, missions like *XMM-Newton*, *Chandra*, *NuSTAR*, *Swift*, and *Fermi*, just to cite some of them, have provided a large amount of data to study a number of astrophysical systems. For instance, X-ray and γ-ray radiation is emitted by material orbiting in the strong gravity region of black holes and can be used to study the physical properties of these objects as well as their astrophysical environment. The next generation of satellites, like *eXTP* and *ATHENA*, promises to provide unprecedented high-quality data to investigate a number of open questions about the physics and the astrophysics of the Universe.

Despite the importance of X-ray and γ-ray astronomy in modern physics and astrophysics, as well as the non-small communities working in this field, a manual for beginners, as well as a comprehensive reference for researchers, covering the main techniques of X-ray and γ-ray data reduction and analysis is missing in the literature. In most cases, one has to refer to online material spread over the web, and to rely on the help of advisors or colleagues.

The ambition of the present book is thus to try to provide a compact pedagogical manual on X-ray and γ-ray astronomy, where one can find all the necessary materials to quickly start to work in the field, and, in particular, to study black holes and the physical phenomena occurring in their strong gravity region. The book starts with a brief review on black holes and the emission mechanisms responsible for the generation of X-ray and γ-ray radiation. Then we discuss the observational facilities in X-ray and γ-ray astronomy, and how they work. The last part of the book is devoted to the discussion of X-ray and γ-ray data reduction and analysis. The book should provide the basic tools to be able to write a scientific paper with the material obtained after the analysis of a source.

Shanghai, China
January 2020

Cosimo Bambi

Contents

Contributors

William Alston Institute of Astronomy, Cambridge, UK

Cosimo Bambi Department of Physics, Fudan University, Shanghai, China

Peter Boorman Astronomical Institute, Academy of Sciences, Prague, Czech Republic;
Faculty of Physical Sciences and Engineering, Department of Physics & Astronomy, University of Southampton, Southampton, UK

Andrea Bulgarelli INAF OAS Bologna, Bologna, Italy

Valentina Fioretti INAF OAS Bologna, Bologna, Italy

Matteo Guainazzi European Space Agency, ESTEC, Noordwijk, The Netherlands

Jiachen Jiang Department of Astronomy, Tsinghua Univerisity, Beijing, China

Vinay L. Kashyap Center for Astrophysics, Harvard & Smithsonian, Cambridge, MA, USA

Sourabh Nampalliwar Theoretical Astrophysics, Eberhard-Karls Universität Tübingen, Tübingen, Germany

Michael Parker European Space Agency (ESA), European Space Astronomy Center (ESAC), Madrid, Spain

Dheeraj R. Pasham MIT Kavli Institute for Astrophysics and Space Research, MIT, Cambridge, MA, USA

Chapter 1
Fundamental Concepts

Cosimo Bambi and Sourabh Nampalliwar

1.1 Introduction

Beginning with the special theory of relativity in 1905, Albert Einstein soon realized that Newton's theory of gravity had to be superseded, to harmonize the equivalence principle and the special theory of relativity. After numerous insights, false alarms, and dead ends, the theory of general relativity was born in 1915 [14]. It took some years for it to take over Newton's theory as the leading framework for the description of gravitational effects in our Universe, and over the past century, it has become one of the bedrocks of modern physics.

Just a year after its proposition, Karl Schwarzschild was able to find an exact solution in general relativity, much to the surprise of Einstein himself, who only had approximate solutions by that time. The Schwarzschild solution [23] turned out to be much more astrophysically relevant than anyone could have imagined, and describes the simplest class of *black holes*[1] in Einstein's theory.

Roughly speaking, a black hole is a region in which gravity is so strong that nothing, not even light, can escape. A boundary, known as the *event horizon*, separates the interior of the black hole from the exterior region and acts as a one-way membrane:

[1] The origin of the term black hole is quite intriguing. While it is not clear who used the term first, it appeared for the first time in a publication in the January 18, 1964 issue of Science News Letter. It was on a report on a meeting of the American Association for the Advancement of Science by journalist Ann Ewing. The term became quickly very popular after it was used by John Wheeler at a lecture in New York in 1967.

C. Bambi (✉)
Department of Physics, Fudan University, 2005 Songhu Road,
Shanghai 200438, China
e-mail: bambi@fudan.edu.cn

S. Nampalliwar
Theoretical Astrophysics, Eberhard-Karls Universität Tübingen,
Auf der Morgenstelle 10, 72076 Tübingen, Germany
e-mail: sourabh.nampalliwar@uni-tuebingen.de

© Springer Nature Singapore Pte Ltd. 2020

C. Bambi (ed.), *Tutorial Guide to X-ray and Gamma-ray Astronomy*,
https://doi.org/10.1007/978-981-15-6337-9_1

particle and radiation can enter the black hole but cannot exit from it. Remarkably, a primitive concept of black hole was already discussed at the end of the 18th century in the context of Newtonian mechanics by John Michell and Pierre-Simon Laplace. The starting point was the corpuscular theory of light developed in the 17th century. Here light is made of small particles traveling with a finite velocity, say c. Michell and Laplace noted that the escape velocity from the surface of a body of mass M and radius R exceeds c if $R < R_{\rm crit}$, where

$$R_{\rm crit} = \frac{2G_{\rm N}M}{c^2} \tag{1.1}$$

and $G_{\rm N}$ is Newton's gravitational constant. If such a compact object were to exist, it should not be able to emit radiation from its surface and should thus look black. This was the conclusion of Michell and Laplace and these objects were called dark stars.

The Schwarzschild type black holes are described by just one parameter, the *mass*, and it is the characteristic quantity setting the size of the system. The *gravitational radius* of an object of mass M is defined as

$$r_{\rm g} = \frac{G_{\rm N}M}{c^2} = 14.77 \left(\frac{M}{10\ M_\odot}\right)\ {\rm km}\ . \tag{1.2}$$

The associated characteristic time scale is

$$\tau = \frac{r_{\rm g}}{c} = 49.23 \left(\frac{M}{10\ M_\odot}\right) \mu{\rm s}\ . \tag{1.3}$$

For a 10 $M_\odot$ black hole, $r_{\rm g} \sim 15$ km and $\tau \sim 50\,\mu$s. We can thus expect that physical phenomena occurring around a similar object can have a variability timescale of the order of 0.1–1 ms. For a black hole with $M \sim 10^6\ M_\odot$, we find $r_{\rm g} \sim 10^6$ km and $\tau \sim 5$ s, so physical processes occurring near its gravitational radius can have a variability timescale of the order of 10–100 s. For the most supermassive black holes with $M \sim 10^9\ M_\odot$, we have $r_{\rm g} \sim 10^9$ km and $\tau \sim 1$ h.

The astrophysical implications of such black hole solutions were not taken very seriously for a long time. For example, influential scientists like Arthur Eddington argued that "some unknown mechanism" had to prevent the complete collapse of a massive body and the formation of a black hole in the Universe. The situation changed only in the 1960s with the advent of X-ray observations. Yakov Zel'dovich and, independently, Edwin Salpeter were the first, in 1964, to propose that quasars were powered by central supermassive black holes [22, 26]. In the early 1970s, Thomas Bolton and, independently, Louise Webster and Paul Murdin identified the X-ray source Cygnus X-1 as the first stellar-mass black hole candidate [10, 25]. The uncertainty of those times can be imagined by the scientific wager between Kip Thorne and Stephen Hawking, the latter claiming that Cygnus X-1 was in fact not a black hole. Hawking conceded the bet in 1990. In the past few decades, a large

number of astronomical observations have pointed out the existence of stellar-mass black holes in some X-ray binaries [20] and of supermassive black holes at the center of many galaxies [17]. Thanks to X-ray and γ-ray missions like *XMM-Newton*, *Chandra*, *NuSTAR*, *Swift*, and *Fermi*, in the past 20 years there has been substantial progress in the study of these objects. In September 2015, the LIGO experiment detected, for the first time, the gravitational waves emitted from the coalescence of two black holes [1].

1.2 Black Holes in General Relativity

In 4-dimensional general relativity, black holes are relatively simple objects, in the sense that they are completely characterized by a small number of parameters: the mass M, the spin angular momentum J, and the electric charge Q. This is the result of the *no-hair theorem*, which holds under specific assumptions [12, 13, 16, 21]. The name "no-hair" refers to the fact black holes have only a small number of features (hairs). Violations of the no-hair theorem are possible in the presence of exotic fields, extra dimensions, or extensions of general relativity.

A *Schwarzschild black hole* is a spherically symmetric, non-rotating, and electrically uncharged black hole and is completely characterized by its mass. In the presence of a non-vanishing electric charge, we have a *Reissner-Nordström black hole*, which is completely specified by two parameters and describes a spherically symmetric and non-rotating black hole of mass M and electric charge Q. A *Kerr black hole* is an uncharged black hole of mass M and spin angular momentum J. The general case is represented by a *Kerr-Newman black hole*, which has a mass M, a spin angular momentum J, and an electric charge Q.

Astrophysically, black holes are expected to belong to the Kerr family. After the collapse of a massive body and the creation of an event horizon, the gravitational field of the remnant quickly reduces to that of a Kerr black hole by emitting gravitational waves [18, 19]. For astrophysical macroscopic objects, the electric charge is extremely small and can be ignored [2, 4]. The presence of an accretion disk around the black hole, as well as of stars orbiting the black hole, do not appreciably change the strong gravity region around the compact object [5–7]. Astrophysical black holes should thus be completely specified by their mass and spin angular momentum. It is often convenient to use the dimensionless spin parameter a_* instead of J. For a black hole of mass M and spin J, a_* is defined as

$$a_* = \frac{cJ}{G_{\rm N} M^2} \,. \tag{1.4}$$

In general relativity, the choice of the coordinate system is arbitrary, and therefore the numerical values of the coordinates have no physical meaning. Nevertheless, they can often provide the correct length or time scale of the system. In Boyer–Lindquist coordinates, the typical coordinate system for Kerr black holes, the radius of the

event horizon is

$$r_{\rm H} = r_{\rm g} \left(1 + \sqrt{1 - a_*^2} \right) , \tag{1.5}$$

and depends on M (via $r_{\rm g}$ and a_*) and J (via a_*). The radius of the event horizon thus ranges from $2\,r_{\rm g}$ for a non-rotating black hole to $r_{\rm g}$ for a maximally rotating ($a_* = \pm 1$) black hole. Note that Eq. (1.5) requires that $|a_*| \leq 1$. Indeed for $|a_*| > 1$ there is no black hole and the Kerr solution describes the gravitational field of a *naked singularity*. In the context of astrophysical observations, the possibility of the existence of naked singularity is usually ignored, and this is also motivated by the considerations that (*i*) there is no known mechanism capable of creating a naked singularity, and (*ii*) even if created, the spacetime is likely unstable (for more details, see for instance Ref. [2]).

The properties of equatorial circular orbits around a black hole are important for astrophysical observations because they describe the orbits of the particles in a putative accretion disk around the compact object. In Newtonian mechanics, equatorial circular orbits (i.e. orbits in the plane perpendicular to the spin of the object) around a point-like object are always stable. However, this is not true for equatorial circular orbits around a Kerr black hole. Here we have the existence of an *innermost stable circular orbit*, often abbreviated to ISCO. In Boyer–Lindquist coordinates, the ISCO radius is [8]

$$\begin{aligned} r_{\rm ISCO} &= r_{\rm g} \left[3 + Z_2 \mp \sqrt{(3 - Z_1)\,(3 + Z_1 + 2 Z_2)} \right] , \\ Z_1 &= 1 + \left(1 - a_*^2\right)^{1/3} \left[(1 + a_*)^{1/3} + (1 - a_*)^{1/3} \right] , \\ Z_2 &= \sqrt{3 a_*^2 + Z_1^2} \, . \end{aligned} \tag{1.6}$$

The ISCO radius turns out to be $6\,r_{\rm g}$ for a Schwarzschild black hole and move to $r_{\rm g}$ ($9\,r_{\rm g}$) for a maximally rotating black hole and a corotating (counterrotating) orbit, namely an orbit with angular momentum parallel (antiparallel) to the black hole spin. Figure 1.1 shows the radial values of the event horizon $r_{\rm H}$ and of the ISCO radius $r_{\rm ISCO}$ in Boyer–Lindquist coordinates as a function of the black hole spin parameter a_*.

1.3 Black Holes in Astrophysics

While we cannot observe any kind of radiation (neither electromagnetic, nor gravitational) from the region inside the event horizon, astrophysical black holes can be studied by detecting the electromagnetic and gravitational radiation produced in the vicinity of the event horizon. Gravitational radiation is generated by the interaction of matter/energy and the spacetime, and its frequency depends on the size of the system. In particular, the wavelength roughly scales as the linear size of the system

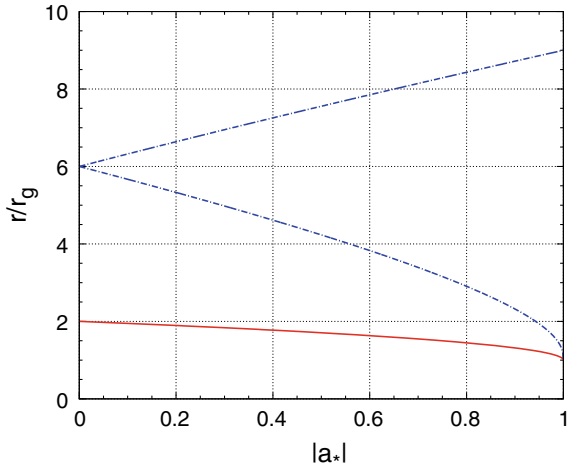

Fig. 1.1 Radius of the event horizon (red solid line) and of the ISCO (blue dash-dotted line) of a Kerr black hole in Boyer–Lindquist coordinates as a function of the spin parameter a_*. For the ISCO radius, the upper curve refers to counterrotating orbits and the lower curve to corotating orbits

emitting gravitational radiation. Gravitational radiation from black holes is expected to range from a few nHz, in the case of the merger of galaxies with supermassive black holes at their respective centers, to a few kHz, in the case of the merger and ringdown of stellar-mass black holes. Radiation of different wavelengths require different observational facilities to be detected.

Electromagnetic radiation can be emitted by the gas in the accretion disk, jet, and outflows, as well as by possible bodies (like stars) orbiting the black hole (see Fig. 1.2). The electromagnetic spectra of astrophysical black holes range from the radio to the γ-ray band (see Table 1.1 for the list of the bands of the electromagnetic spectrum). The photon energy is determined by the emission mechanism and the black hole environment. Photons with different wavelengths carry different information about the black hole and its environment, and require different observational facilities to be detected. Table 1.2 lists the possible components of the electromagnetic spectrum of a black hole system (more details on each component will be provided in the next chapter).

Among the various astrophysical processes, accretion onto a black hole can be an extremely efficient mechanism to convert mass into energy. If $\dot{M}$ is the mass accretion rate, the total power of the accretion process can be written as

$$P = \eta \dot{M} c^2 \,, \tag{1.7}$$

where η is the total efficiency. In general, the energy released in the accretion process will be converted into radiation and kinetic energy of jets/outflows, so we can write

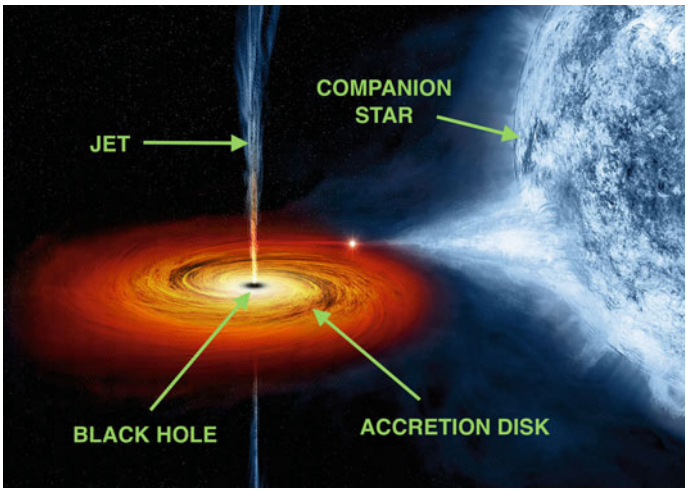

Fig. 1.2 An artist's illustration of Cygnus X-1. The stellar-mass black hole pulls material from a massive, blue companion star toward it. This material forms an accretion disk around the black hole. We also see a jet originating from the region close to the black hole. Credit: NASA

Table 1.1 Bands of the electromagnetic spectrum. Note that different authors may use slightly different definitions

Band	Wavelength	Frequency	Energy
Radio	$> 0.1\,\mathrm{m}$	$< 3\,\mathrm{GHz}$	$< 12.4\,\mu\mathrm{eV}$
Microwave	1 mm–0.1 m	3–300 GHz	12.4 μeV–1.24 meV
Infrared (IR)	700 nm–1 mm	300 GHz–430 THz	1.24 meV–1.7 eV
Visible	400–700 nm	430–790 THz	1.7–3.3 eV
Ultraviolet (UV)	10–400 nm	$7.9 \cdot 10^{14}$–$3 \cdot 10^{16}$ Hz	3.3–124 eV
X-Ray	0.01–10 nm	$3 \cdot 10^{16}$–$3 \cdot 10^{19}$ Hz	124 eV–124 keV
γ-Ray	< 0.01 nm	$> 3 \cdot 10^{19}$ Hz	> 124 keV

$$\eta = \eta_{\rm r} + \eta_{\rm k}\,, \tag{1.8}$$

where $\eta_{\rm r}$ is the radiative efficiency and can be measured from the bolometric luminosity $L_{\rm bol}$ from the equation $L_{\rm bol} = \eta_{\rm r} \dot{M} c^2$ if the mass accretion rate is known, and $\eta_{\rm k}$ is the fraction of gravitational energy converted into kinetic energy of jets/outflows. The actual efficiency depends on the morphology of the accretion flow. In the case of a Novikov–Thorne disk (see Sect. 2.3.1), the accretion disk is on the black hole equatorial plane, perpendicular to the spin of the compact object. The particles of the gas follow equatorial circular orbits, they lose energy and angular momentum, and they move to smaller and smaller radii. When the particles reach the ISCO radius, they quickly plunge onto the black hole, without significant emission of additional radiation. The efficiency of the process is thus given by

Table 1.2 Summary of the possible sources of electromagnetic radiation in black hole systems and typical energy bands for stellar-mass and supermassive black holes. For soft X-ray we mean the X-ray band below a few keV. Cold material orbiting the compact object and not belonging to the accretion disk is common in supermassive black holes: the emission lines can be narrow (broad) if the material is far (near) the compact object and moving with low (high) speed

Source	Emission	Stellar-mass black holes	Supermassive black holes
Accretion disk	Thermal	UV to soft X-ray	Visible to UV
Accretion disk	Reflection spectrum	X-ray	X-ray
Corona	Inverse compton	X-ray and γ-ray	X-ray and γ-ray
Jet	Synchrotron	Radio to soft X-ray	Radio to soft X-ray
Jet	Inverse Compton	X-ray and γ-ray	X-ray and γ-ray
Cold material	Emission lines	–	IR to X-ray
Companion star	Thermal	Visible and UV	–

$$\eta_{\rm NT} = 1 - E_{\rm ISCO}\,, \tag{1.9}$$

where $E_{\rm ISCO}$ is the specific energy of the gas at the ISCO radius, namely the energy per unit mass of the gas. For a Kerr black hole, the specific energy of a particle orbiting an equatorial circular orbit at the Boyer–Lindquist radial coordinate r is [2]

$$E = \frac{r^{3/2} - 2r_{\rm g}r^{1/2} \pm a_* r_{\rm g}^{3/2}}{r^{3/4}\sqrt{r^{3/2} - 3r_{\rm g}r^{1/2} \pm 2a_* r_{\rm g}^{3/2}}}\,. \tag{1.10}$$

If we plug the radial coordinate of the ISCO radius in Eq. (1.6), we find that the efficiency of the process is around 5.7% for a Schwarzschild black hole and monotonically increases (decreases) as the spin parameter increases (decreases) up to about 42.3% (3.8%) for $a_* = 1$ ($a_* = -1$):

$$\begin{aligned}
\eta_{\rm NT}(a_* = 0) &= 1 - \frac{2\sqrt{2}}{3} \approx 0.057\,,\\
\eta_{\rm NT}(a_* = 1) &= 1 - \frac{1}{\sqrt{3}} \approx 0.423 \quad \text{(corotating disk)}\,,\\
\eta_{\rm NT}(a_* = -1) &= 1 - \frac{5}{\sqrt{27}} \approx 0.038 \quad \text{(counterrotating disk)}\,.
\end{aligned} \tag{1.11}$$

Figure 1.3 shows $\eta_{\rm NT}$ as a function of the spin parameter a_* for corotating (upper curve) and counterrotating (lower curve) disks. The efficiency of a Novikov–Thorne disk can be compared to other astrophysical processes. For instance, if we consider nuclear reactions inside the Sun, the main process is the fusion of protons to form helium-4 nuclei. The total mass of the final state is lower than the total mass of the initial state, and this difference is released into energy (electromagnetic radiation and

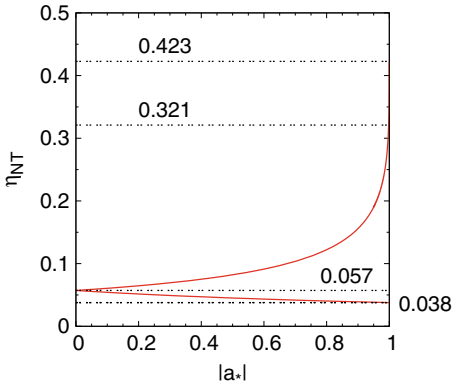

Fig. 1.3 Efficiency of a Novikov–Thorne disk $\eta_{\rm NT}$ as a function of the spin parameter a_* for Kerr black holes. The upper (lower) curve is for corotating (counterrotating) orbits. The dotted horizontal lines mark the radiative efficiencies for $a_* = 1$ ($\eta_{\rm NT} \approx 0.423$), $a_* = 0.998$ ($\eta_{\rm NT} \approx 0.321$), $a_* = 0$ ($\eta_{\rm NT} \approx 0.057$), and $a_* = -1$ ($\eta_{\rm NT} \approx 0.038$)

kinetic energy of the particles in the final state). The efficiency of the process is only around 0.7%, namely about 0.7% of the initial mass is converted into energy.

If the mass accretion rate is low and the accreting gas has a low angular momentum, the efficiency of the accretion process can be much smaller than 1, $\eta \ll 1$, because the particles of the gas simply fall onto the gravitational well of the black hole without releasing much electromagnetic radiation. Very low efficiencies are also possible in the case of very high mass accretion rate, and in this case it is because the particle density of the accretion flow is too high and the medium becomes optically thick to the radiation emitted by the gas, so everything is advected onto the black hole and lost after crossing the event horizon. An important concept in this regard is the *Eddington luminosity*. The concept is actually more general, and the Eddington luminosity refers to the maximum luminosity for an object, not necessarily a black hole. The Eddington luminosity $L_{\rm Edd}$ is reached when the pressure of the radiation luminosity on the emitting material balances the gravitational force towards the object. If a normal star has a luminosity $L > L_{\rm Edd}$, the pressure of the radiation luminosity drives an outflow. If the luminosity of the accretion flow of a black hole exceeds $L_{\rm Edd}$, the pressure of the radiation luminosity stops the accretion process, reducing the luminosity. Assuming that the emitting medium is a ionized gas of protons and electrons, the Eddington luminosity of an object of mass M is

$$L_{\rm Edd} = \frac{4\pi G_{\rm N} M m_p c}{\sigma_{\rm Th}} = 1.26 \cdot 10^{38} \left(\frac{M}{M_\odot}\right) \text{ erg/s}\,, \tag{1.12}$$

where m_p is the proton mass and $\sigma_{\rm Th}$ is the electron Thomson cross section. For an accreting black hole, we can define the Eddington mass accretion rate $\dot{M}_{\rm Edd}$ from

$$L_{\rm Edd} = \eta_{\rm r} \dot{M}_{\rm Edd} c^2 \,, \tag{1.13}$$

where $\eta_{\rm r}$ is still the radiative efficiency.

1.4 X-Ray and γ-Ray Observatories

Our focus in this book is X-rays and γ-rays. There are a number of astrophysical sources emitting X-ray (0.1–100 keV) and γ-ray (>100 keV) radiation, such as galaxy clusters, compact objects, supernova remnants, and stars. X-ray radiation can be emitted by hot gas (10^6–10^9 K) or generated by bremsstrahlung, synchrotron processes, inverse Compton scattering, fluorescent emission, and nuclear decay. γ-ray radiation can be generated by the same processes at higher energies, as well as by electron-positron annihilation. As a back-of-the-envelope estimate, consider an electromagnetic particle falling onto a black hole, beginning from infinity at rest. In Newtonian mechanics, the energy of a particle is the sum of its kinetic and potential energy, and the sum is zero if the particle is at rest at infinity

$$E = \frac{1}{2} m v^2 - G_{\rm N} \frac{M m}{r} \approx 0 \,, \tag{1.14}$$

where m and v are the mass and the velocity of the particle falling onto the black hole and M is the black hole mass. At the radial coordinate $r \sim 10\, r_{\rm g}$, the kinetic energy of the particle is around 10% of its rest mass, namely around 100 MeV for protons and 50 keV for electrons. We can thus expect the emission of radiation with such an energy, which is indeed in the X-ray and γ-ray bands.

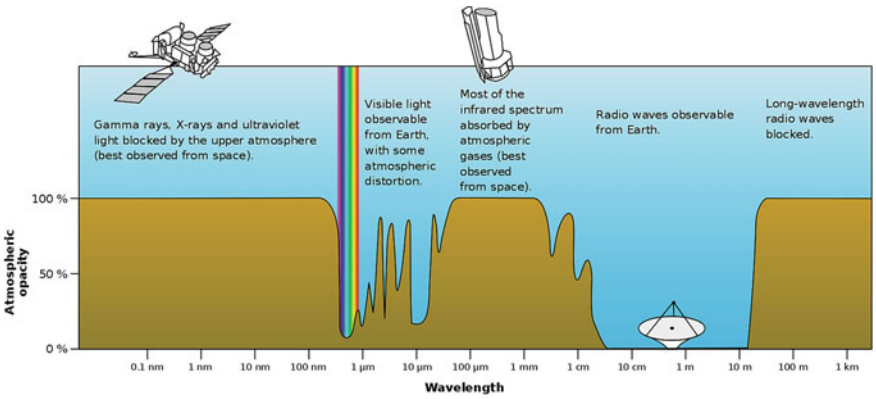

Fig. 1.4 Atmospheric opacity as a function of photon wavelength. Since the atmosphere is opaque at most wavelengths, only optical and radio telescopes can be at ground level on Earth. γ-ray, X-ray, UV, and IR observational facilities are required to be on board of rockets or satellites. Credit: NASA

A large part of the electromagnetic spectra is blocked by the Earth's atmosphere, see Fig. 1.4. If it were not so, life on Earth—at least as we know—would be impossible, because γ-rays, X-rays, and UV photons are harmful for any organism. To be able to observe X-rays and γ-rays, observatories must thus be on board rockets or satellites. The first X-ray observatory can be considered a V2 rocket launched in 1948, which was used to observe the Sun, the brightest X-ray source in the sky. The first extrasolar X-ray source was discovered in 1962 by a team led by Riccardo Giacconi with an X-ray detector on board of an Aerobee 150 sounding rocket [15]. The source, known as Scorpius X-1, is an X-ray binary with a neutron star of 1.4 $M_\odot$ and a companion of 0.42 $M_\odot$. Giacconi received the Nobel Prize in Physics in 2002 for pioneering the research field today called X-ray astronomy. Since the discovery of Scorpius X-1, a steady progress in technology, theory and analysis, has made X-ray astronomy a leading scientific field in astrophysics research. Tables 1.3 and 1.4 present some of the most important X-ray and γ-ray observatories from past, present, and future.

1.5 Open Problems and Future Directions

X-ray and γ-ray radiation have provided invaluable information about black holes and their astrophysical environments and breakthroughs in fundamental physics. In the case of accreting black holes, we can study of the accretion process in the strong gravity region, how the gas falls onto the compact object, and how jets and outflows are generated. In the past 10–15 years, a few X-ray techniques have been developed to measure black hole spins, and before the detection of gravitational waves these were the only techniques capable of measuring black hole spins.

While several puzzles have been answered, many new ones have appeared and remain unresolved. Some of them are as follows:

1. While Einstein's general relativity is the standard framework for describing the gravitational features in our Universe, several shortcomings of the theory have led to the development of a large number of modified theories of gravity. The techniques used for measuring black hole spin can also be used to test the motion of particle in the strong gravity region around black holes from modified theories of gravity and be used to perform precision tests of general relativity [2, 3, 11, 24].
2. There are a number of dark matter models predicting the production of γ-rays from dark matter particle annihilation or decay. The study of the γ-ray spectrum of astrophysical sites where there may be a large amount of dark matter particles is an indirect search for dark matter. If we detect an excess of γ-rays with respect to that expected from the pure astrophysical environment, as well as some specific feature in the γ-ray spectrum, this may be interpreted as an indirect evidence of dark matter particles.
3. What is the spin distribution among stellar-mass and supermassive black holes and how does the spin distribution change over cosmological times? In the case

Table 1.3 List of some of the most important X-ray missions from past, present, and future

Mission	Launch date	End of mission	Instruments
PAST			
Röntgensatellit (ROSAT)	1990	1999	XRT (0.1–2 keV)
Advanced Satellite for Cosmology and Astrophysics (ASCA)	1993	2000	GIS (0.7–10 keV) SIS (0.4–10 keV)
Rossi X-ray Timing Explorer (RXTE)	1995	2012	ASM (2–10 keV) PCA (2–60 keV) HEXTE (15–250 keV)
Suzaku	2005	2015	XRS (0.3–12 keV) XIS (0.2–12 keV) HXD (10–600 keV)
Hitomi	2016	2016	SXS (0.4–12 keV) SXI (0.3–12 keV) HXI (5–80 keV)
PRESENT			
Chandra X-ray Observatory (CXO)	1999	–	ACIS (0.2–10 keV) HRC (0.1–10 keV) LETG (0.08–2 keV) HETG (0.4–10 keV)
XMM-Newton	1999	–	EPIC-MOS (0.15–15 keV) EPIC-pn (0.15–15 keV) RGS (0.33–2.5 keV)
International Gamma-Ray Astrophysics Laboratory (INTEGRAL)	2002	–	IBIS (15 keV–10 MeV) SPI (18 keV–8 MeV) JEM-X (3–35 keV)

(continued)

of supermassive black holes, the spin distribution would also provide information about the evolution of their host galaxies [9].

4. What is the mechanism responsible for the production of jets in black holes?
5. What is the mechanism responsible of the observed quasi-periodic oscillations (QPOs) in the X-ray power density spectrum of black holes? Can we use QPOs for measuring black hole spins and test general relativity?
6. What is the exact origin of supermassive black holes and how do they grow so fast? In particular, we know supermassive black holes of billions of Solar masses at redshifts higher than 6 and we do not have a clear understanding of how such objects were created and were able to grow so fast in a relatively short time.

Table 1.3 (continued)

Mission	Launch date	End of mission	Instruments
Swift	2004	–	BAT (15–150 keV) XRT (0.2–10 keV)
Monitor of All-sky X-ray Image (MAXI)	2009	–	SSC (0.5–10 keV) GSC (2–30 keV)
Nuclear Spectroscopic Telescope Array (NuSTAR)	2012	–	FPMA (3–79 keV) FPMB (3–79 keV)
ASTROSAT	2015	–	SXT (0.3–80 keV) LAXPC (3–80 keV) CZTI (100–300 keV)
Neutron star Interior Composition Explorer (NICER)	2017	–	XTI (0.2–12 keV)
Hard X-ray Modulation Telescope (HXMT)	2017	–	HE (20–250 keV) ME (5–30 keV) LE (1–15 keV)
Spektrum-Roentgen-Gamma (Spektr-RG)	2019	–	eROSITA (0.3–10 keV) ART-XC (0.5–11 keV)
FUTURE			
X-Ray Imaging and Spectroscopy Mission (XRISM)	2022	–	Resolve (0.4–12 keV) Xtend (0.3–12 keV)
Enhanced X-ray Timing Polarization (eXTP)	2027	–	SFA (0.5–20 keV) LAD (1–30 keV)
Advanced Telescope for High Energy Astrophysics (ATHENA)	2031	–	X-IFU (0.2–12 keV) WFI (0.1–15 keV)

7. How does the host environment determine the properties of supermassive black holes? And how do supermassive black holes determine the properties of their host environment?
8. Do intermediate mass black holes exist? Do small primordial black holes created in the early Universe exist?

Table 1.4 List of some of the most important γ-ray missions from past and present

Mission	Launch date	End of mission	Instruments
PAST			
GRANAT	1989	1999	SIMGA (30–1300 keV) PHEBUS (0.1–100 MeV) KONUS-B (0.01–8 MeV) TOURNESOL (0.002–20 MeV)
Compton Gamma Ray Observatory (CGRO)	1991	2000	OSSE (0.06–10 MeV) COMPTEL (0.8–30 MeV)) EGRET (20–3000 MeV) BATSE (0.015–110 MeV)
PRESENT			
International Gamma-Ray Astrophysics Laboratory (INTEGRAL)	2002	–	SPI (0.02–8 MeV) IBIS (0.015–10 MeV)
Swift	2004	–	BAT (15–150 keV)
Astrorivelatore Gamma ad Immagini LEggero (AGILE)	2007	–	GRID (30 MeV–50 GeV) MC (0.25–200 MeV)
Fermi gamma ray space telescope	2008	–	LAT (20 Mev–300 GeV) GBM (8 keV–30 MeV)

References

1. B.P. Abbott et al., LIGO scientific and virgo collaborations. Phys. Rev. Lett. **116**, 061102 (2016). arXiv:1602.03837 [gr-qc]
2. C. Bambi, *Black Holes: A Laboratory for Testing Strong Gravity*, (Springer, Singapore, 2017). https://doi.org/10.1007/978-981-10-4524-0
3. C. Bambi, Rev. Mod. Phys. **89**, 025001 (2017). arXiv:1509.03884 [gr-qc]
4. C. Bambi, A.D. Dolgov, A.A. Petrov, JCAP **0909**, 013 (2009). arXiv:0806.3440 [astro-ph]
5. C. Bambi, D. Malafarina, N. Tsukamoto, Phys. Rev. D **89**, 127302 (2014). arXiv:1406.2181 [gr-qc]
6. C. Bambi et al., Universe **4**, 79 (2018). arXiv:1806.02141 [gr-qc]
7. E. Barausse, V. Cardoso, P. Pani, Phys. Rev. D **89**, 104059 (2014). arXiv:1404.7149 [gr-qc]
8. J.M. Bardeen, W.H. Press, S.A. Teukolsky, Astrophys. J. **178**, 347 (1972)
9. E. Berti, M. Volonteri, Astrophys. J. **684**, 822 (2008). arXiv:0802.0025 [astro-ph]
10. C.T. Bolton, Nature **235**, 271 (1972)
11. Z. Cao, S. Nampalliwar, C. Bambi, T. Dauser, J.A. Garcia, Phys. Rev. Lett. **120**, 051101 (2018). arXiv:1709.00219 [gr-qc]
12. B. Carter, Phys. Rev. Lett. **26**, 331 (1971)
13. P.T. Chrusciel, J.L. Costa, M. Heusler, Living Rev. Rel. **15**, 7 (2012). arXiv:1205.6112 [gr-qc]
14. A. Einstein, Annalen Phys. **49**, 769 (1916); Annalen Phys. **14**, 517 (2005)
15. R. Giacconi, H. Gursky, F.R. Paolini, B.B. Rossi, Phys. Rev. Lett. **9**, 439 (1962)

16. W. Israel, Phys. Rev. **164**, 1776 (1967)
17. J. Kormendy, D. Richstone, Ann. Rev. Astron. Astrophys. **33**, 581 (1995)
18. F. Pretorius, Phys. Rev. Lett. **95**, 121101 (2005). arXiv:gr-qc/0507014
19. R.H. Price, Phys. Rev. D **5**, 2419 (1972)
20. R.A. Remillard, J.E. McClintock, Ann. Rev. Astron. Astrophys. **44**, 49 (2006). arXiv:astro-ph/0606352
21. D.C. Robinson, Phys. Rev. Lett. **34**, 905 (1975)
22. E.E. Salpeter, Astrophys. J. **140**, 796 (1964)
23. K. Schwarzschild, Sitzungsber. Preuss. Akad. Wiss. Berlin (Math. Phys.) **1916**, 189 (1916) arXiv:physics/9905030
24. A. Tripathi, S. Nampalliwar, A.B. Abdikamalov, D. Ayzenberg, C. Bambi, T. Dauser, J.A. Garcia, A. Marinucci, Astrophys. J. **875**, 56 (2019). arXiv:1811.08148 [gr-qc]
25. B.L. Webster, P. Murdin, Nature **235**, 37 (1972)
26. Y.B. Zeldovich, Dokl. Akad. Nauk **155**, 67 (1964); Sov. Phys. Dokl. **9**, 195 (1964)

Chapter 2
Accreting Black Holes

Sourabh Nampalliwar and Cosimo Bambi

2.1 Theory of Black Holes: Formation and Masses

Black holes happen to be surprisingly simple objects. Only two parameters, the *mass* M and the *spin* J, are thought to be sufficient to characterize a black hole in our Universe [11]. The spin parameter cannot be arbitrary and must satisfy the constraint $J/M^2 \leq 1$, which is the condition for the existence of the event horizon, as shown in Eq. (1.5). There are no theoretical constraints on the value of the mass of a black hole, which may thus be arbitrarily small as well as arbitrarily large.

From astronomical observations, we have strong evidence of two classes of astrophysical black holes:

1. *Stellar-mass black holes* [126], with masses $\sim 3-100 M_\odot$.
2. *Supermassive black holes* [72], with masses $> 10^5 M_\odot$.

One would expect, and there is some evidence, that black holes with masses in the intermediate range should exist [29]. These are termed *intermediate-mass black holes*. Each of these classes is theorized to have a different past, present and future. We will discuss them separately.

2.1.1 Stellar-Mass Black Holes

The most common formation channel for stellar-mass black holes is gravitational collapse. In lay terms, when a star runs out of fuel, the pressure inside is insufficient to hold the star against gravitational pull and the star collapses. For massive enough stars, the star collapses all the way to a singularity and a black hole is born.

S. Nampalliwar (✉)
Theoretical Astrophysics, Eberhard-Karls Universität Tübingen,
Auf der Morgenstelle 10, 72076 Tübingen, Germany
e-mail: sourabh.nampalliwar@uni-tuebingen.de

C. Bambi
Department of Physics, Fudan University, 2005 Songhu Road, Shanghai 200438, China
e-mail: bambi@fudan.edu.cn

© Springer Nature Singapore Pte Ltd. 2020

C. Bambi (ed.), *Tutorial Guide to X-ray and Gamma-ray Astronomy*,
https://doi.org/10.1007/978-981-15-6337-9_2

The initial mass of a stellar-mass black hole depends on the properties of the progenitor: its mass, its evolution, and the supernova explosion mechanism [15]. Depending on these details, the supernova remnant could be a neutron star, where the quantum neutron pressure can hold against the gravitational collapse, or a black hole. In fact, the lower bound on the black hole initial mass may come from the maximum mass for a neutron star: the exact value is currently unknown, since it depends on the equation of state of matter at super-nuclear densities, but it should be in the range of $2-3\ M_\odot$. It is possible though, that a mass gap exists between the most massive neutron stars and the less massive black holes [36]. An upper bound on stellar-mass black holes may be derived from the progenitor's metallicity. The final mass of the remnant is determined by the mass loss rate by stellar winds, which increases with the metallicity because heavier elements have a larger cross section than lighter ones, and therefore they evaporate faster. For a low-metallicity progenitor [59, 60, 138], the mass of the black hole remnant may be $M \lesssim 50\ M_\odot$ or $M \gtrsim 150\ M_\odot$. As the metallicity increases, black holes with $M \gtrsim 150\ M_\odot$ disappear, because of the increased mass loss rate. Note, however, that some models do not find remnants with a mass above the gap, because stars with $M \gtrsim 150\ M_\odot$ may undergo a runaway thermonuclear explosion that completely destroys the system, without leaving any black hole remnant [59, 60]. Stellar-mass black holes may thus have a mass in the range of $3-100\ M_\odot$. Until now, all the known stellar-mass black holes in X-ray binaries have a mass $M \approx 3-20\ M_\odot$ [25]. Gravitational waves, on the other hand, have shown the existence of heavier stellar-mass black holes. In particular, the event called GW150914 was associated with the coalescence of two black holes with masses $M \approx 30\ M_\odot$ that merged to form a black hole with $M \approx 60\ M_\odot$ [1].

From stellar evolution studies, we expect that in our Galaxy there is a population of 10^8–10^9 black holes formed at the end of the evolution of heavy stars [155, 159], and the same number can be expected in similar galaxies. But with observations, we only know about 20 black holes with a dynamical measurement of the mass and about 50 without (it is thus possible that some of them are not black holes but neutron stars). This is because their detection is very challenging. The simplest scenario is when the black hole is in a binary system and has a companion star. The presence of a compact object can be discovered from the observation of a short timescale variability, the non-detection of a stellar spectrum, etc. The study of the orbital motion of the companion star can permit the measurement of the mass function [25]

$$f(M) = \frac{K_c^3 P_{\rm orb}}{2\pi G_N} = \frac{M \sin^3 i}{(1+q)^2}\,, \tag{2.1}$$

where $K_c = v_c \sin i$, v_c is the velocity of the companion star, i is the angle between the normal of the orbital plane and our line of sight, $P_{\rm orb}$ is the orbital period of the system, $q = M_c/M$, M_c is the mass of the companion, and M is the mass of the dark object. If we can somehow estimate i and M_c, we can infer M, and in this case we talk about dynamical measurement of the mass. The dark object is a black hole if $M > 3\ M_\odot$ [65, 76, 128].

Note that, among astronomers, it is common to call "black hole" a compact object for which there is a dynamical measurement of its mass proving that $M > 3\,M_\odot$. The latter indeed guarantees that the object is too heavy for being a neutron star. "Black hole candidates" are instead compact objects that are supposed to be black holes, for instance because of the detection of spectral features typical of black holes, but for which there is no dynamical measurement of their mass.

Black holes in X-ray binaries (black hole binaries[1]) are grouped into two classes: *low-mass X-ray binaries* (LMXBs) and *high-mass X-ray binaries* (HMXBs). Here, "low" and "high" refers to the stellar companion, not to the black hole: in the case of LMXBs, the companion star normally has a mass $M_c < 3\,M_\odot$, while for HMXBs the companion star has $M_c > 10\,M_\odot$. Observationally, we can classify black hole binaries either as *transient X-ray sources* or *persistent X-ray sources*. LMXBs are usually transient sources, because the mass transfer is not continuous (for instance, at some point the surface of the companion star may expand and the black hole strips some gas): the system may be bright for a period ranging from some days to a few months and then be in a quiescent state for months or even decades. Every year we discover 1–2 new objects, when they pass from their quiescent state to an outburst (see Sect. 2.4.1). Overall, we expect 10^3–10^4 LMXBs in the Galaxy [66, 176]. HMXBs are persistent sources: the mass transfer from the companion star to the black hole is a relatively regular process (typically it is due to the stellar wind of the companion) and the binary is a bright source at any time without quiescent periods. Figure 2.1 shows 22 X-ray binaries with a stellar-mass black hole confirmed by dynamical measurements. To have an idea of the size of these systems, the figure also shows the Sun (whose radius is 0.7 million km) and the distance Sun-Mercury (about 50 million km). The black holes have a radius <100 km and cannot be seen, but we can clearly see their accretion disks formed from the transfer of material from the companion star. The latter may have a quite deformed shape (in particular, we can see some cusps) due to the the tidal force produced by the gravitational field of the black hole. Among the sources listed in the figure, Cygnus X-1 (Cyg X-1 in Fig. 2.1), LMC X-1, LMC X-3, and M33 X-7 are HMXBs, while all other systems are LMXBs. Among these HMXBs, only Cygnus X-1 is in our Galaxy. Among the LMXBs, there is GRS 1915+105, which is quite a peculiar source: since 1992, it is a bright X-ray source in the sky, so it can be considered a persistent source. This is probably because of its large accretion disk, which can provide enough material at any time.

Black holes in compact binary systems (black hole-black hole or black hole-neutron star) can be detected with gravitational waves when the signal is sufficiently strong. Figure 2.2 shows the first detections by the LIGO/Virgo collaboration. The name of the event is classified as GW (gravitational wave event) and then the date of detection: for example, GW150914 was detected on 14 September 2015. LVT151012

[1] Generally speaking, a *black hole binary* is a binary system in which at least one of the two bodies is a black hole, and a *binary black hole* is a binary system of two black holes.

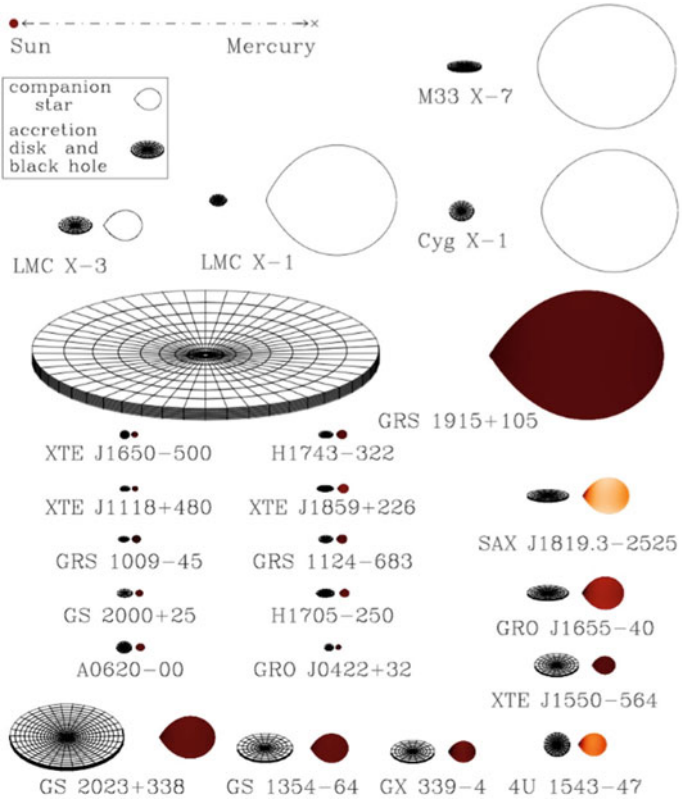

Fig. 2.1 Sketch of 22 X-ray binaries with a stellar-mass black hole confirmed by dynamical measurements. For every system, the black hole accretion disk is on the left and the companion star is on the right. The color of the companion star roughly indicates its surface temperature (from brown to white as the temperature increases). The orientation of the disks indicates the inclination angles of the binaries. For comparison, in the top left corner of the figure we see the system Sun-Mercury: the distance between the two bodies is about 50 million km and the radius of the Sun is about 0.7 million km. Figure courtesy of Jerome Orosz

is not classified as a gravitational wave event because the signal to noise ratio was not large enough to qualify as a detection.[2] For every event, the figure shows the two original black holes as well as the final one after merger.

Isolated black holes are much more elusive. In principle, they can be detected by observing the modulation of the light of background stars due to the gravitational lensing caused by the passage of a black hole along the line of sight of the observer [8].

[2]LVT stands for LIGO/Virgo transient.

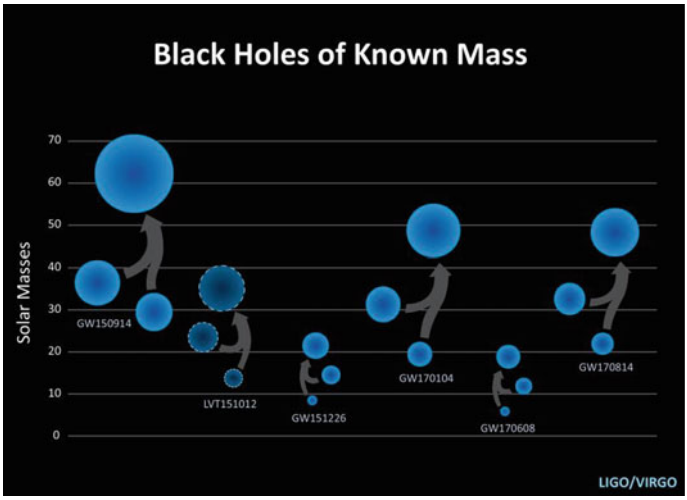

Fig. 2.2 Masses of the first black holes observed with gravitational waves, with the two initial objects merging into a larger one, as shown by the arrows. Image Credit: LIGO/NSF/Caltech/SSU Aurore Simmonet

2.1.2 Supermassive Black Holes

The formation channels of supermassive black holes are not well established. The gigantic masses of supermassive black holes are not thought to be natal, but acquired. Accretion has been shown to be an effective mechanism for growing the masses of black holes. In fact, some models suggest the possibility of super-Eddington accretion, and this may indeed be a possible path to the rapid growth of supermassive black holes [82]. Another possibility is merger of several black holes. But the question of the progenitor, or *seed*, remains open. See [162] for a review of the possible formation channels.

Astronomical observations show that at the center of many galaxies there is a large amount of mass in a relatively small volume. The standard interpretation is that these objects are supermassive black holes with $M \sim 10^5$–$10^{10}\ M_\odot$. Strong constraints come from the center of our Galaxy and NGC 4258 [83]. For our Galaxy, we can study the Newtonian motion of individual stars and infer that at the center there is an object with a mass of $4 \cdot 10^6\ M_\odot$ (see Fig. 2.3). An upper bound on the size of this body can be obtained from the minimum distance approached by one of these stars, which is less than 45 AU and corresponds to $\sim$1,200 r_g for a $4 \cdot 10^6\ M_\odot$ object. In the end, we can exclude the existence of a cluster of compact non-luminous bodies like neutron stars and therefore we can conclude that the most natural interpretation is that it is a supermassive black hole. In the case of NGC 4258, we can study the orbital motion of gas in the nucleus, and again we can conclude that the central object is too massive, compact, and old to be a cluster of neutron stars. In the case of other galaxies, it is not possible to put such constraints with the available data, but it is thought that

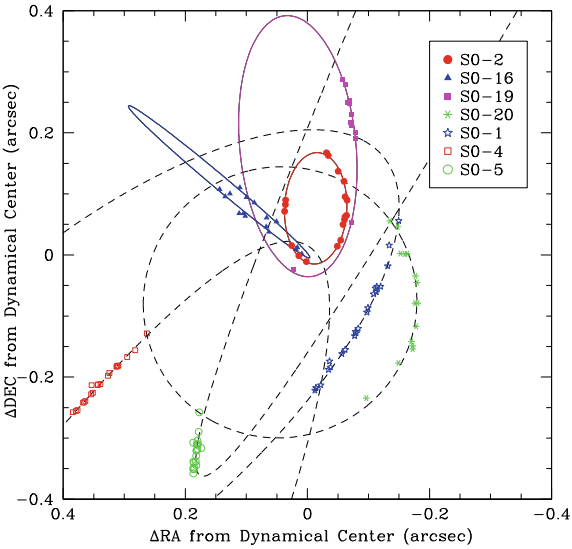

Fig. 2.3 Astrometric positions and orbital fits for seven stars orbiting the supermassive black hole at the center of the Milky Way. From [50]. ©AAS. Reproduced with permission

every mid-size (like the Milky Way) or large galaxy has a supermassive black hole at its center.[3] For smaller galaxies, the situation is more uncertain. Most models predict supermassive black holes at the center of lighter galaxies as well [162], but there exist predictions of faint low-mass galaxies with no supermassive black hole at their centers [163, 164]. Observations suggest that some small galaxies have a supermassive black hole and other small galaxies do not [39, 44].

2.1.3 Intermediate-Mass Black Holes

Intermediate-mass black holes are, by definition, black holes with a mass between the stellar-mass and the supermassive ones, say $M \sim 10^2$–$10^5\ M_\odot$. At the moment, there is no dynamical measurement of the mass of these objects, and their actual nature is still controversial. Among the possible formation channels, intermediate-mass black holes are expected to form at the center of dense stellar clusters, by mergers.

Observational evidence for intermediate-mass black holes is inconclusive. The presence of an intermediate-mass black hole at the center of stellar clusters should increase the velocity dispersion in the cluster. Some studies suggest that there are indeed intermediate-mass black holes at the center of certain globular clusters [48, 49]. Some intermediate-mass black hole candidates are associated with ultra luminous X-ray sources [28]. These objects have an X-ray luminosity $L_X > 10^{39}$ erg/s, which exceeds the Eddington luminosity of a stellar-mass object, and they may thus

[3] Exceptions may be possible: the galaxy A2261-BCG has a very large mass but it might not have any supermassive black hole at its center [118].

have a mass in the range 10^2–$10^5\ M_\odot$. However, we cannot exclude the possibility that they are actually stellar-mass black holes (or neutron stars [10]) with non-isotropic emission and a moderate super-Eddington mass accretion rate [109]. The existence of intermediate-mass black holes is also suggested by the detection of some quasi-periodic oscillations (QPOs, see Sect. 2.5.3) in some ultra-luminous X-ray sources. QPOs are currently not well understood, but they are thought to be associated to the fundamental frequencies of the oscillation of a particle around a black hole. Since the size of the system scales as the black hole mass, QPOs should scale as $1/M$, and some observations indicate the existence of compact objects with masses in the range 10^2–$10^5\ M_\odot$ [114].

2.2 Theory of Black Holes: Evolution and Spins

Apart from mass, a typical black hole is expected to have some spin. Generally speaking, the value of the spin parameter of a black hole can be expected to be determined by the competition of three physical processes: the event creating the object, mergers, and gas accretion.

2.2.1 Stellar-Mass Black Holes

In the case of black hole binaries, it is usually thought that the spin of a black hole is mainly natal and that the effect of the accretion process is negligible [67]. The argument is that a stellar-mass black hole has a mass around $10\ M_\odot$. If the stellar companion is a few Solar masses, the black hole cannot significantly change its mass and spin angular momentum even after swallowing the whole star. If the stellar companion is heavy, its lifetime is too short: even if the black hole accretes at the Eddington rate, there is not enough time to transfer the necessary amount of matter to significantly change the black hole spin parameter. One may expect that a black hole cannot swallow more than a few $M_\odot$ from the companion star, and for a $10\ M_\odot$ object this is not enough to significantly changes a_* [67]. If the black hole spin were mainly natal, its value should be explained by studying the gravitational collapse of massive stars. While there are still uncertainties in the angular momentum transport mechanisms of the progenitors of stellar-mass black holes, it is widely accepted that the gravitational collapse of a massive star with Solar metallicity cannot create fast-rotating remnants [172, 175]. The birth spin of these black holes is expected to be low (see e.g. [42] and references therein).

Observations of spins of stellar-mass black holes contradict the above hypothesis. For instance, in the case of LMXBs, the black hole in GRS 1915+105 has $a_* > 0.98$ [89] and $M = 12.4 \pm 2.0\ M_\odot$ [120], while the stellar companion's mass is $M = 0.52 \pm 0.41\ M_\odot$. In the case of HMXBs, the black hole in Cygnus X-1 has $a_* > 0.98$ [55, 56] and $M = 14.8 \pm 1.0\ M_\odot$, while the stellar wind from the companion is

not an efficient mechanism to transfer mass. Very high spin values are also measured for 4U 1630-472, GS 1354-645, MAXI J1535-571, and Swift J1658.2, see Table 2.2. While black holes in LMXBs and HMXBs should form in different environments, in both cases the origin of so high spin values is puzzling. In [42], the authors show that at least in the case of LMXBs, the accretion process immediately after the formation of a black hole binary may be very important and be responsible for the observed high spins. For HMXBs, possible channels for producing high spins are discussed in [119].

2.2.2 Supermassive Black Holes

The case of supermassive black holes in galactic nuclei is different. The initial value of their spin parameter is likely completely irrelevant: their mass has increased by several orders of magnitude from its original value, and the spin parameter has evolved accordingly.

There are two primary channels of mass acquisition for supermassive black holes, mergers and accretion. On average, the capture of small bodies (*minor merger*) in randomly oriented orbits should spin the black hole down, since the magnitude of the orbital angular momentum for corotating orbits is always smaller than the one for counterrotating orbits [62]. In the case of random merger of two black holes with comparable mass (*major merger*), the most probable final product is a black hole with $a_* \approx 0.70$, while fast-rotating objects with $a_* > 0.9$ should be rare [17]. On the other hand, accretion from a disk can potentially be a very efficient way to spin a compact object up[4] [17]. In this case, black holes in active galactic nuclei (AGNs) may have a spin parameter close to the Thorne limit (see next section). Such a possibility seems to be supported by some observations; see e.g. [170] and also the spin measurements from X-ray reflection spectroscopy in Table 2.3.

2.2.3 Thorne Limit

An accreting black hole changes its mass M and spin angular momentum J as it swallows more and more material from its disk. In the case of a Novikov–Thorne disk (see next section), it is relatively easy to calculate the evolution of these parameters. If we assume that the gas in the disk emits radiation until it reaches the radius of the innermost stable circular orbit (ISCO) and then quickly plunges onto the black hole, the evolution of the spin parameter a_* is governed by the following equation [154]

[4]Unless the accretion proceeds via short episodes (chaotic accretion) [69], in which case it is effectively like minor mergers.